KEYPOINT-BASED STEREOPHOTOCLINOMETRY

Travis Driver[1*], Andrew Vaughan[2], Yang Cheng[2], Adnan Ansar[2], John Christian[1], and Panagiotis Tsiotras[1];
[1]Georgia Institute of Technology, Atlanta, GA, [2]Jet Propulsion Laboratory, California Institute of Technology, Pasadena, CA. [*][travisdriver@gatech.edu]

Abstract. *This paper proposes the incorporation of techniques from stereophotoclinometry (SPC) in a structure-from-motion (SfM) system to estimate the surface normal and albedo at detected landmarks. In contrast to the traditional SPC paradigm, which relies on human-in-the-loop verification and a priori information to achieve accurate results, we forego the expensive maplet estimation step and instead leverage dense keypoint correspondences from a deep learning-based keypoint detection and matching method to provide the photogrammetric constraints. The proposed framework is validated on imagery of the Cornelia crater on Asteroid 4 Vesta.*

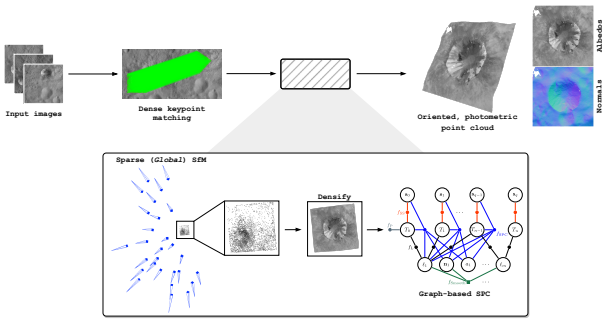

Figure 1. System overview.

Introduction. Missions to to small bodies (e.g., asteroids, comets) currently rely on an extended characterization phase, where a shape model is reconstructed from images acquired during a ground-controlled trajectory around the body. Shape models are essential for characterizing the body and estimating the spacecraft's relative pose in subsequent phases.[1] However, the current shape reconstruction method, stereophotoclinometry (SPC), relies on humans-in-the-loop and accurate *a priori* information to ensure accurate results. Specifically, SPC attempts to estimate a collection of digital terrain maps (DTMs), high-resolution local topography and albedo maps, through direct alignment of ortho-rectified projections, or *orthoimages*, of a given surface patch from multiple images predicated on an initial shape model and accurate *a priori* estimates of the spacecraft's pose (position and orientation). Photometric stereo techniques are applied to derive surface gradients and albedos of the imaged surface patches at each pixel of the orthoimages. The local topography solution is fixed upon convergence, typically requiring human input to achieve precise alignment to the images, and used to refine pose and landmark estimates through a multistep iterative process by rendering the DTM and aligning it across multiple views.[1]

In contrast to the traditional SPC approach, this work proposes to combine dense keypoint correspondences from recently proposed "detector-free" matching methods, i.e., DKM,[2] with photometric stereo constraints and Sun vector measurements in a Structure-from-Motion (SfM) system to estimate surface normals and albedos at estimated landmarks. The proposed framework (illustrated in Fig. 1), which leverages *factor graphs*[3] to model and solve the complex SPC estimation problem, forgoes the expensive local maplet estimation step, eliminates reliance on *a priori* information, and streamlines the optimization process. We apply the proposed framework to *real* imagery of the Cornelia crater on Asteroid 4 Vesta, demonstrating precise alignment to an SPC derived map.

Small Body Photometry. Photometric stereo (PS) is the process of determining surface gradients and albedos of an object by observing it from different viewpoints and lighting conditions and is leveraged by SPC to facilitate dense surface reconstruction. Let an image taken at time index k be denoted by $I_k \colon \Omega_k \to \mathbb{R}_+$ over the pixel domain $\Omega_k \subset \mathbb{R}^2$. The measured image brightness $\hat{I}_k(\mathbf{p}_{j,k})$ (in units of I/F) at a keypoint $\mathbf{p}_{j,k} \in \Omega_k$ associated with a landmark $\boldsymbol{\ell}_j \in \mathbb{R}^3$ can be modeled by

$$I(\alpha_{j,k}, \beta_{j,k}, \phi_{j,k}, a_j) = a_j \Lambda(\phi_{j,k}) \left((1 - g(\phi_{j,k})) \cos\alpha_{j,k} + g(\phi_{j,k}) \frac{2\cos\alpha_{j,k}}{\cos\alpha_{j,k} + \cos\beta_{j,k}} \right), \tag{1}$$

where a_j is the albedo at landmark $\boldsymbol{\ell}_j$ and $\alpha_{j,k}$, $\beta_{j,k}$, and $\phi_{j,k}$ are the incidence, emission, and phase angles, respectively, at landmark $\boldsymbol{\ell}_j$ in the k^{th} image. The *phase function*, $\Lambda(\phi) = \sum_{i=0}^{4} B_i \phi^i$, describes the changes in brightness with phase that are independent of $\alpha_{j,k}$ and $\beta_{j,k}$, and the combination of Lambert and Lommel-Seeliger photometric functions are weighted according to $g(\phi) = C_0 + C_1\phi$, as proposed by Schröder et al.[4]

The Sun-relative direction $\mathbf{s}_k^{\mathcal{B}} \in \mathbb{S}^2$ in I_k, expressed in a body-fixed frame of the small body $\mathcal{B}$, can be estimated using measurements from typical onboard instrumentation (e.g., Sun sensors, star trackers). The emitted light vector $\mathbf{e}_{k,j}^{\mathcal{B}} = \mathbf{r}_{\mathrm{C}_k\mathrm{B}}^{\mathcal{B}} - \boldsymbol{\ell}_j^{\mathcal{B}}$ can be determined from the estimates of $T_{\mathcal{B}\mathcal{C}_k} \in \mathrm{SE}(3)$, i.e., the transformation from the camera frame $\mathcal{C}_k$ to $\mathcal{B}$, and $\boldsymbol{\ell}_j^{\mathcal{B}}$ provided by SfM. Finally, dropping the superscripts and letting T_k denote $T_{\mathcal{B}\mathcal{C}_k}$ for conciseness, Equation (1) can be written in terms of T_k, $\mathbf{s}_k$, and the surface normal $\mathbf{n}_j \in \mathbb{S}^2$ at $\boldsymbol{\ell}_j$ (also expressed in $\mathcal{B}$) by noticing that $\cos\alpha_{j,k} = \mathbf{s}_k^\top \mathbf{n}_j$, $\cos\beta_{j,k} = \mathbf{e}_{k,j}^\top \mathbf{n}_j / \|\mathbf{e}_{k,j}\|$, and $\phi_{j,k} = \cos^{-1}\left(\mathbf{s}_k^\top \mathbf{e}_{k,j} / \|\mathbf{e}_{k,j}\|\right)$. We can now define a factor f_{SPC} corresponding to the presented PS constraints (assuming

zero-mean Gaussian noise) as follows:

$$f_{\text{SPC}}(T_k, \mathbf{s}_k, \boldsymbol{\ell}_j, \mathbf{n}_j, a_j; \Sigma_k) \propto \exp\left\{-\frac{1}{2}|I(T_k, \mathbf{s}_k, \boldsymbol{\ell}_j, \mathbf{n}_j, a_j) - \hat{I}_k(\hat{\mathbf{p}}_{j,k})|^2_{\Sigma_k}\right\}. \quad (2)$$

This allows for estimation of $\mathbf{n}_j$ and a_j using the measurements $\hat{I}_k(\hat{\mathbf{p}}_{j,k})$, while also further constraining the landmark's position $\boldsymbol{\ell}_j$, Sun-relative direction $\mathbf{s}_k$, and the position of the spacecraft $\mathbf{r}_{\text{C}_k\text{B}}$.

Sun Vector Measurements. Our framework assumes knowledge of the Sun-relative direction $\mathbf{s}_k$, which can be measured directly by a Sun sensor. We assume that the measurements $\hat{\mathbf{s}}^{\mathcal{C}}_k \in \mathbb{S}^2$ are available at each time index k and are expressed in the camera frame $\mathcal{C}$. Recalling that T_k denotes $T_{\mathcal{BC}_k}$ and $\mathbf{s}_k$ is expressed in the $\mathcal{B}$ frame, a measurement prediction function $\mathbf{s}^{C}(T_k, \mathbf{s}_k)$ can be defined to predict the measured incident light direction $\hat{\mathbf{s}}^{\mathcal{C}}$ in the $\mathcal{C}$ frame from the current estimates of T_k and $\mathbf{s}_k$, i.e., $\mathbf{s}^{\mathcal{C}}(T_k, \mathbf{s}_k) \triangleq R^{-1}_{\mathcal{BC}_k}\mathbf{s}_k$. We define a factor f_{SS} to incorporate (simulated) Sun sensor measurements into the estimation problem as follows:

$$f_{\text{SS}}\left(T_k, \mathbf{s}_k; \Sigma_{j,k}\right) \propto \exp\left\{-\frac{1}{2}\|\mathbf{s}^{\mathcal{C}}(T_k, \mathbf{s}_k) - \hat{\mathbf{s}}^{\mathcal{C}}_k\|^2_{\Sigma_{j,k}}\right\}. \quad (3)$$

This further constrains the orientation of the camera $R_{\mathcal{BC}_k}$ and the Sun-relative direction $\mathbf{s}_k$.

Local Smoothness Constraints. While the photometric minimization and Sun vector terms modeled by f_{SPC} and f_{SS}, respectively, are sufficient to estimate the surface normal and albedo, Horn[5] indicates that the solution tends to be unstable and gets stuck in local minima. Thus, Horn proposed the use of local smoothness constraints which minimize the "departure from smoothness." We define smoothness constraint *factors* as follows:

$$f_{\text{Smooth}}\left(\boldsymbol{\ell}_j, \mathbf{n}_j, \boldsymbol{\ell}_{j'}; \eta\right) \propto \exp\left\{-\frac{\eta}{2}\left|\cos^{-1}\left(\mathbf{d}^{\top}_{j',j}\mathbf{n}_j\right) - 90^\circ\right|^2\right\}, \quad (4)$$

where η weights the local smoothness penalty, and $\mathbf{d}_{j',j} = (\boldsymbol{\ell}_{j'} - \boldsymbol{\ell}_j)/\|\boldsymbol{\ell}_{j'} - \boldsymbol{\ell}_j\|$.

Experimental Setup. Our experiments leverage imagery of the Cornelia crater on Asteroid 4 Vesta captured by NASA's Dawn mission for evaluation of the proposed approach. We compare our pipeline against four different baselines: the SPC solution, two different methods based on stereophotogrammetry (SPG), and the dense SfM solution (i.e., the proposed method without the SPC factors). The root mean squared error between the measured, $\hat{I}_k(\hat{\mathbf{p}}_{j,k})$, and estimated, $I(T_k, \mathbf{s}_k, \boldsymbol{\ell}_j, \mathbf{n}_j, a_j)$, image brightness, normalized by the average measured brightness, is taken to be the *photometric error*.[4] The *landmark error* is the distance between the estimated landmark and the closest point in the baseline map (after alignment), the *normal error* is the angle between the estimated and baseline normal vectors, and the *albedo error* is the percent error between the estimated and baseline albedos.

Implementation Details. Keypoint measurements and matches are computed using DKM,[2] which provides dense, per-pixel correspondences. The 2,048 most confident DKM correspondences are input to the Georgia Tech Structure-from-Motion (GTSfM) library to generate the initial sparse SfM solution. Image brightness values are (bilinearly) interpolated at the keypoints to derive the measurements $\hat{I}_k(\hat{\mathbf{p}}_{j,k})$ used in the proposed SPC factors. The image brightness measurements are assigned a standard deviation of $\sigma_I = 0.01$. The surface normals are initialized by finding the 32 closest neighbors to each point in the point cloud and fitting a plane to this local terrain, and the normal to the plane is taken as the initial surface normal. Next, these initial surface normals are then used to initialize the albedo by independently computing the albedo in each image and taking the average.

The smoothness factors are inserted into the graph according to the keypoints in the reference image (corresponding to $k = 0$). Specifically, a smoothness factor is inserted between a landmark, $\boldsymbol{\ell}_j$ (and its associated surface normal, $\mathbf{n}_j$) and a neighboring landmark, $\boldsymbol{\ell}_{j'}$, if $\|\hat{\mathbf{p}}_{j,0} - \hat{\mathbf{p}}_{j',0}\| \leq 1$. We found a very small value for the local smoothness weight to work well for our experiment, where we used a value of $\eta = 10^{-4}$. We leverage the GTSAM library[3] to model the proposed approach using factor graphs and optimize the resulting nonlinear least-squares using the Levenberg-Marquardt algorithm.

Results. The resulting albedos, surface normals, and photometric errors from our proposed SPC-SfM solution are provided in Figure 2, where we achieve a mean photometric error of ∼1%. Next, we compare our solution to the SPC reconstruction in Fig. 3. We are able to achieve average normal errors of $< 5^\circ$ and albedo errors of $< 4\%$. However, our solution exhibits regions with relatively large landmark errors. Yet, these large landmark error regions are not present when comparing against the SfM and SPG solutions, as shown in Fig. 4. This suggests that the errors in the landmarks arise from errors in the SPC solution, as opposed to our approach, purportedly due to errors in the associated surface normal. Indeed, since the map heights in the traditional SPC solution are computed by integrating the slopes, errors in the slope translate to errors in the landmark positions that propagate from the points in the map where the slope errors arise towards the direction of the integration.

Acknowledgments. This work was supported by a NASA Space Technology Graduate Research Opportunity. A portion of this research was carried out at the Jet Propulsion Laboratory, California Institute of Technology, under a contract with the National Aeronautics and Space Administration (80NM0018D0004).

References.

[1] R. Gaskell et al., "Stereophotoclinometry on the OSIRIS-REx mission: Mathematics and methods," *The Planetary Science J.*, vol. 4, no. 4, 2023.

[2] J. Edstedt, I. Athanasiadis, M. Wadenbäck, and M. Felsberg, "DKM: Dense kernelized feature matching for geometry estimation," in *CVPR*, pp. 17765–17775, 2023.

[3] F. Dellaert, "Factor graphs and GTSAM: A hands-on in-

troduction," Tech. Rep. GT-RIM-CP&R-2012-002, Georgia Institute of Technology, 2012.

[4] S. Schröder, S. Mottola, H. Keller, C. Raymond, and C. Russell, "Resolved photometry of Vesta reveals physical properties of crater regolith," *P&SS*, vol. 85, pp. 198–213, 2013.

[5] B. K. Horn, "Height and gradient from shading," *Int. J. of Computer Vision (IJCV)*, vol. 5, no. 1, pp. 37–75, 1990.

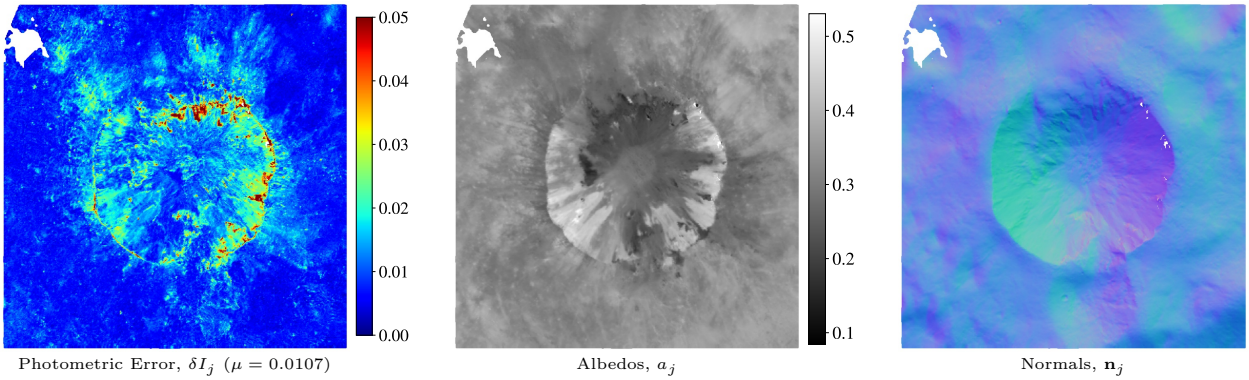

Figure 2. Reconstructed surface normal and albedo maps and photometric errors.

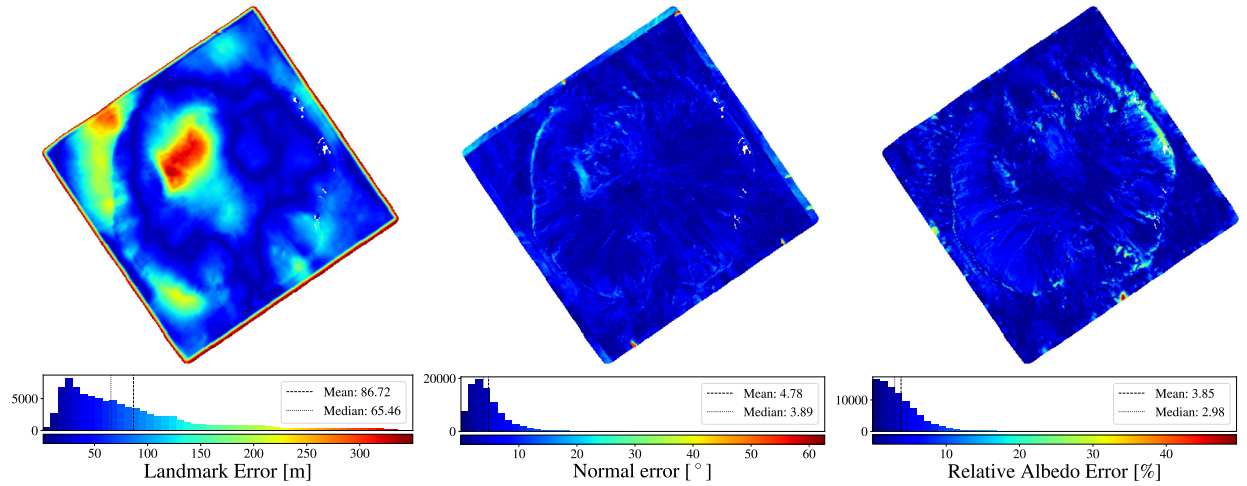

Figure 3. Quantitative comparison between our solution and the SPC baseline with respect to landmark error, normal error, and relative albedo error.

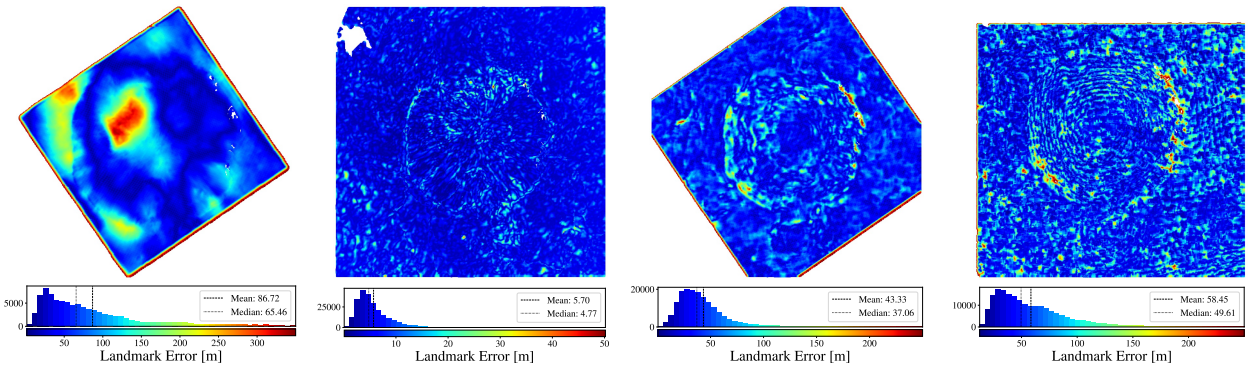

Figure 4. Quantitative comparison between our solution and the SPC, SfM, and SPG solutions with respect to landmark error.